Journal of Integrative Neuroscience, Vol. 6, No. 3 (2007) 447–476

Imperial College Press
www.icpress.co.uk

Special Report

A MODEL OF GRID CELLS INVOLVING EXTRA HIPPOCAMPAL PATH INTEGRATION, AND THE HIPPOCAMPAL LOOP

P. GAUSSIER*, J. P. BANQUET†, F. SARGOLINI‡, C. GIOVANNANGELI*, E. SAVE‡ and B. POUCET‡

*Neuro-Cybernetic Team, Image and Signal Processing Lab. (ETIS)
Cergy Pontoise University and ENSEA
6 av du Ponceau
95014 Cergy Pontoise, France

†Neurosciences and Modelisation Institute
INSERM 742, UPMC
Jussieu, Paris, France

‡LNC (Neurobiology of Cognition Laboratory) —
Université de Provence, Marseille

Received 19 March 2007
Accepted 2 August 2007

In this paper, we present a model for the generation of grid cells and the emergence of place cells from multimodal input to the entorhinal cortex (EC). In this model, grid cell activity in the dorsocaudal medial entorhinal cortex (dMEC) [28] results from the operation of a long-distance path integration system located outside the hippocampal formation, presumably in retrosplenial and/or parietal cortex. If the connections between these structures and dMEC are organized as a modulo N operator, the resulting activity of dMEC neurons is a grid cell pattern. Furthermore, a robust high-resolution positional code can be built from a small set of different grid cells if the modulo factors are relatively prime. On the other hand, broad visual place cell activity in the MEC can result from the integration of visual information depending on the view-field of the visual input. The merging of entorhinal visual place cell information and grid cell information in the EC and/or in the dentate gyrus (DG) allows the building of precise and robust "place cells" (e.g., whose activity is maintained if light is suppressed for a short duration). Our model supports our previous proposition that hippocampal "place cell" activity code transitions between two successive states ("transition cells") rather than mere current locations. Furthermore, we discuss the possibility that the hippocampal loop participates in the emergence of grid cell activity but is not sufficient by itself. Finally, path integration at a short time scale (which is reset from one place to the next) would be merged in the subiculum with CA3/CA1 "transition cells" [22] to provide a robust feedback about current action to the deep layer of the entorhinal cortex in order to predict the recognition of the new animal location.

Keywords: Grid cells; path integration; entorhinal cortex; hippocampus; place cells; transition cells; vision.

1. Introduction

The core of the present paper is a new model of grid cell activity recorded in the dorsocaudal Medial Entorhinal Cortex dMEC [18, 28, 57]. The model derives from our long-standing modeling efforts using computer simulations and robotics experiments to build "minimal" models accounting for many behaviors. Our modeling strategy avoids the introduction of a given structure if it is not absolutely necessary to obtain the desired behavior. Hence, we can study the dynamics that can be obtained (or not) from a particular brain architecture (constructivist approach [39, 72]). Basically, the interest of robotics experiments is to show the limitations of a model (proof by failure!) in order to propose more coherent models for a better understanding of the explored brain structures. This approach complements those that are dedicated to the development of realistic and complex brain models (see [53, 64, 61, 37, 36, 8, 16] or [32, 38, 42] for instance).

Here, we applied this strategy to propose a model of grid cell activity based on global path integration information outside the hippocampal system (HS). Our model of grid cells largely relies on rules that were previously used to define broad visual place cells in EC. One such rule is that a generic function of pyramidal neurons in the superficial layers of EC is to receive, compress and merge multimodal information from associative cortical areas. This in turn would allow for the buildup of either visual place cells or grid cells (according to the relevant sensory modality). In the discussion, we examine how our grid cell model can be connected with the hippocampal loop in which presumably CA neurons are special devices that learn to predict multimodal events. We will propose a global model in which the output of the CA1 region is transformed in the subiculum [47] before it returns to the deep layer of the entorhinal cortex to close a loop that integrates dynamic movement representations and static place representations.

2. Modeling Broad Place Cells and Grid Cells Activity in EC

2.1. *Broad place cells from visual information*

In previous work, we developed a model of the hippocampus that allowed controlling mobile robots both for visual navigation tasks [22, 3, 24] and for predicting temporal sequences [2, 21]. To obtain visual place cells (VPC), a panoramic image is analyzed sequentially. An internal attentional mechanism is used to collect an image invariant from its location in the part of the panorama under the spotlight [33]. A simple mechanism merging the "what" and "where" information extracted from the visual flow allows for high-performance homing and route following behaviors. In the model, local views ("what" information) are coded in the perirhinal cortex or in other areas of the ventral visual pathway of the rat temporal cortex [35]. The absolute position of the local views in the rat peripheral space is provided by the parietal cortex through the parahippocampal region ("where" information). The merging of "what" and "where" information, which provides a signature of the

place, is performed either in the entorhinal cortex (on the synapses of pyramidal neurons located in the superficial layer of EC–EC_2) or upstream (for instance in the postrhinal cortex [67, 7, 9]). This merging allows activation of a neuron only when a given local view is recognized under a particular azimuth and/or elevation (multiplicative effect of "and" operator). A dynamical short term memory is then supposed to complement the effect of the sequential exploration and build a global code of the current location. Ultimately, a population of place cells learns such a configuration. A competitive mechanism can be used to select the neuron, or the set of neurons, that best recognizes the current place. Generalization capabilities are possible if the azimuth and the elevation are coded on some neural field using a diffusion mechanism centered on the preferred direction [23]. Figure 1 summarizes the different processing steps used to build visual place cells; the detailed model can be find in [22, 3].

The equations used to build the place code and to compute place cell activity are summarized in B.1 and B.2. Figure 1 shows the activity of five visual place cells recorded while the robot was moving on a straight line on a road near our laboratory building. The activity of the simulated cells, even in outdoor conditions, shows a peak for the learned locations. Moreover, they generalize quite correctly over large distance: two to three meters in indoor environments and 20 to 30 meters outside. Compared to the rat hippocampal place cells, modeled visual place cells have broader fields, thus allowing good generalization. Since the rat presumably has access to the same information, our model of visual place cells could correspond to EC cells with broad place fields [51]. As we previously suggested [22], the existence of such broad fields in EC would explain the sparing of some basic navigation skills after bilateral hippocampal damage [14].

2.2. *Grid cells built from extra hippocampal path integration*

Experimental evidences strongly suggest that grid cell activity in dMEC relies primarily on integration of idiothetic information rather than visual information. Idiothetic information is important for path integration (e.g., navigation in the dark, simple dead reckoning. . .). Recent models explain grid cell activity by assuming the pre-existence of a complete regular map allowing to predict which neurons will fire as a result of the previously activated ones [74, 71, 52]. Grid activity is explained by the folding of a 2-dimensional Cartesian map representing the physical environment (a torus which has the advantage that it avoids the side effects related to the borders of the map). This hypothesis raises several issues related, for example, to the size of the maps and to how a coherent map is built from connected environments that constitute a single entity (merging two maps into a single map). But, more than the problem of using these models for behaviors not directly linked to navigation, they suffer from another important drawback. As pointed out by [6], the continuous attractor model proposed in [17] (see also [40, 56]) works correctly only if the network pattern flows exactly in register with the rat position. In other words, the

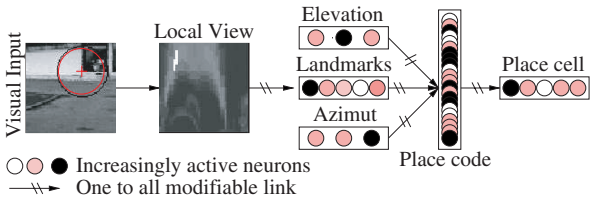

(A)

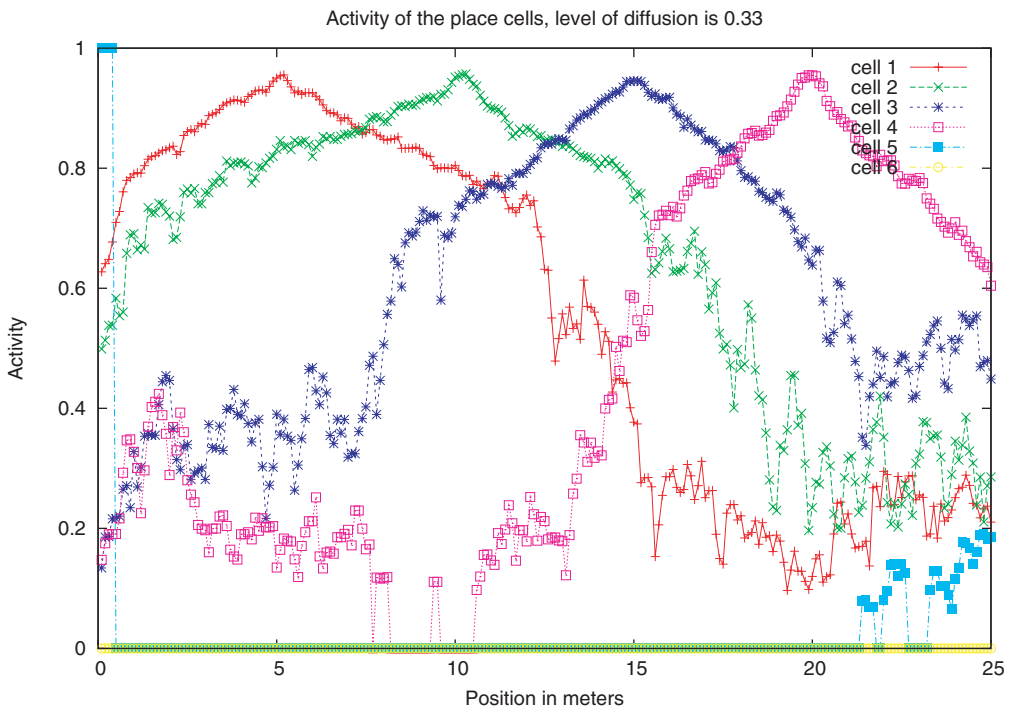

(B)

Fig. 1. (A) Simplified neural network architecture showing the information flow used to build visual place cells. (B) Activity of 6 simulated visual place cells recorded on a linear track in a real outdoor environment. The maximum of activity of the cells is associated with the learned positions. Cell 5 corresponds to a learned place located outside the recording area (on the right). Cell 6 has not be recruited (no learning/null activity).

network must precisely integrate rat velocity (which, in turn, must fit the environment discretization used in the simulation). If speed or movement direction do not correspond exactly to the parameters used for the discretization of the grid (in terms of angle and distance[a]), there is an accumulation of errors inducing a rapid blurring of the grid activity [6] (let us notice this error is not the classical path integration error — both errors will be added!) More importantly, these models also suppose

[a]Distance = speed · time (constant) of the computation time in the hippocampal loop.

that the hippocampus is devoted to navigation: the hippocampus as a cognitive map [31]. To overcome these limitations, we propose that grid cell activity results mainly from the simple projection and merging of a long-distance path integration on the dMEC neurons. This long-distance path integration could be provided by the retrosplenial cortex which is strongly connected with the brain regions involved in spatial signaling [12] and/or by the parietal cortex [49] which receives vestibular information[b] from others cortical areas (the parieto-insular vestibular cortex PIVC [26, 27]). This model contrasts with those computing grid cells (and previously place cells) from the conjunction of a place recognition, a short-distance path integration and finally a head direction system [71, 52, 40, 17] that together allow updating of the rat position from place to place.

Several other models have been proposed to explain how nervous systems of animals and humans could perform the trigonometric computations needed for path integration. Most of these models were first proposed for insect navigation [45, 29, 77] but the principle could apply for mammals. They rely on the general properties of path integration [19, 70, 56, 75]. Our model is directly inspired from Wittman and Etienne [77, 15]. The direction of animal movements are coded on a uniform and circular neural map covering 360° (similar to a 1D neural field [60] except that, for the purpose of simplification there is no dynamical lateral interaction). Each neuron of this map codes for a given direction θ_i relatively to the north (see Appendix A). If the map has N neurons, the angular precision is (360°/N). Based on this coding scheme, vision and motor control can be expressed in the same way, thus allowing the emergence of interesting behaviors by some straightforward connections between the different sensory systems (for instance a visual stimulation under a particular azimuth can trigger the rotation of the animal in the correct direction through one-to-one connections with the motor map). The most active neuron in the path integration layer corresponds to the final direction of the motion since the last reset of the field activity (see Fig. 15 in Appendix A). Its activity level corresponds to the distance traveled in this direction from the starting point. The activity of a given neuron in the field corresponds to the global cosine value in the direction associated to the neuron. For instance, if we consider the neuron associated with the direction $\theta_i = 0$, its activity is $\alpha \sum_{t=t_A}^{t_B} \cos \Phi(t)$ with $\Phi(t)$ the direction of the animal movement at time t. If we also take the neuron associated with direction $\theta_i = \frac{\pi}{2}$, its activity is $\alpha \sum_{t=t_A}^{t_B} \sin \Phi(t)$ (see Eq. (A.3) in Appendix A and replace θ_i by its value). The activity of this pair of neurons corresponds exactly to the (x, y) displacement of the animal from the departure point (supposed to be the reset position of the field). Other pairs of neurons can be used to get the projection of the displacement on nonorthogonal directions. The results are similar if the cosine kernel is replaced by a gaussian or a triangular shape for instance, except that a bias is introduced in the computation [77].

[b]Vestibular lesions disrupt idiothetic navigation or path integration and render navigational behavior critically dependent upon visual cues [65].

Our simplest model of grid cells uses the discretized activities of two of these neurons (associated with two angular positions) to provide a direct measure of the animal displacement in their associated direction. The activity D_i of the neuron associated with direction θ_i is discretized over a new field of neurons E^i_j with $E^i_j = round(\frac{D_i \cdot N_E}{D_{\max}})$ as shown in Fig. 3. $D_{\max}$ is the maximum value of the distance that can be computed by the path integration neural field. N_E is the number of neuron on each field used to discretize the analog value of a given neuron of the path integration neural field. Next a modulo operator allows compressing the discretized activity E^i_j (see Eq. (2.1) and Fig. 3).

$$\begin{aligned} M^n_k &= 1 \quad \text{iff } k = ArgMax(E_j) \bmod MG^n \\ &= 0 \quad \text{otherwise} \end{aligned} \tag{2.1}$$

with MG^n the value of the modulo used to build the nth grid. The computation of the field M^n can be seen as a compression with loss of information of the path integration neural field. As proposed by McNaughton [40], this regular pattern of connections could result from the dynamics of interactions between excitatory and inhibitory recurrent connections, which can create regular Turing structures. Learning the correlations between one path integration stimulus and the grid activity could correspond to the pattern of connections shown in Fig. 2, which represents the modulo operator (Eq. (2.1)). Finally, a self organized group of neurons G^n_l learns the resulting pattern of activity and produces a grid cell activity according to a spatial resolution n defined by the value MG^n. Since, in this model there are only two active inputs, when a neuron learns a particular configuration, the result is equivalent to learn either a "AND" configuration or a response to a product between the two inputs. Hence, the result of the learning can be seen as building the tensorial product $[M_k] \otimes [M_j]$. It is formally equivalent to the *what* $\otimes$ *where* computation used to build our visual place cells. In this model, the absolute difference between ϕ_1 and ϕ_2 determines the value of the grid orientation (Fig. 3). The compression factor of the modulo projection determines the grid spacing. Three prime modulo factors MG^n are sufficient to cover a wide space since the length of the torus corresponds to the product of those prime factors. These numbers do not need to be real prime numbers: they only need to be relatively prime (i.e., three projection groups of

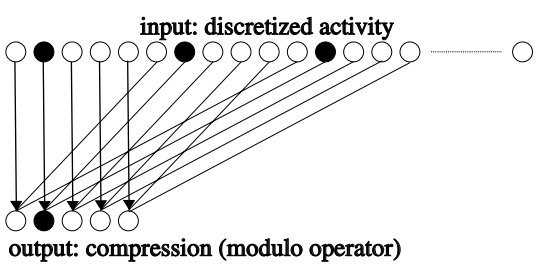

Fig. 2. Simple modulo operator working on a discrete coding of distance projection in a given direction can be the basis of a grid activity.

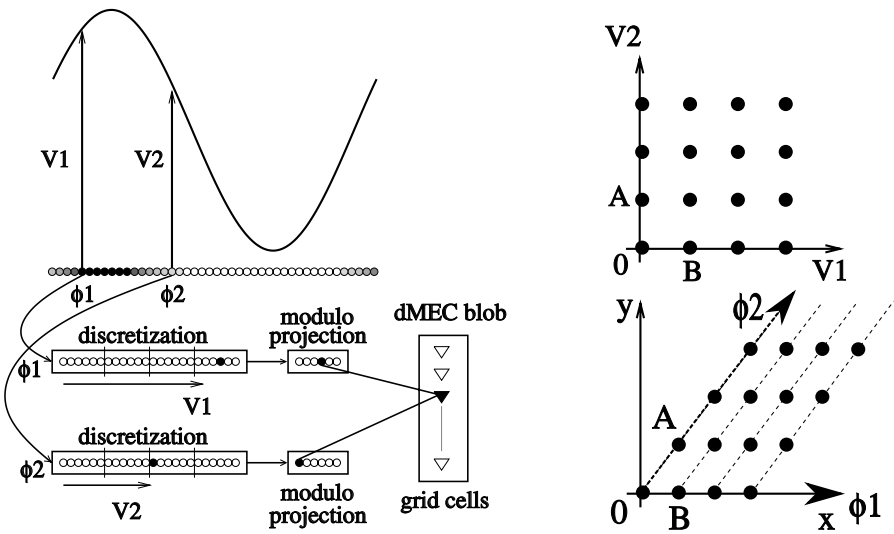

(A) (B)

Fig. 3. (A) Path integration information can be used to build a grid cell activity without the need of a Cartesian coding. The input is a one dimensional neural field used to code the global path integration of the animat. At the level of a dMEC blob, the learning of the conjunction of 2 codes corresponding to the modulo compression of 2 projections of the path integration field is sufficient to obtain grid cells. (B) Selection of the modulo projection in 2 directions ϕ_1 and ϕ_2 determines the grid orientation. The spacing is determined by the modulo value and the radius of the firing field by the discretization factor of the path integration field. All the couples of neurons associated with the same angular difference provide the same grid cell activity.

respectively four, seven and 11 neurons will allow to differentiate the same number of distances than a single linear grid of 240 neurons "$4 \times 7 \times 11 = 308$"). The values of the MG^n factors represent a distance in an abstract unit corresponding to $\frac{D_{\max}}{N_E}$.

Although activity patterns generated by this first simple model resemble grid cell activity at the onset of the experiment, they quickly degrade by spreading over neighboring areas so that ultimately average activity appears almost randomly distributed over space (Fig. 4). This problem is due to the cumulative error in path integration, which depends on the size of the neural field (in our case the use of 121 neurons associated to 121 orientations). A simple solution to this classical drawback [50, 4] is to reset or recalibrate the neural field for path integration at a well know location (e.g., by visual place recognition or visual cues [15]). In the simulation of Fig. 5, path integration is reset when the animat[c] returns (by chance) to a small area defined by strong activation of a given visual place cells.

As a result, the peak size of a grid cell is a direct function of the size of the reset area (recalibration) since reset of global path integration can occur anywhere at the periphery of the visual place cell firing field (the maximum of imprecision corresponds to the diameter of the firing field). Figure 5 shows the region where

[c]Animat = Animal automata [41].

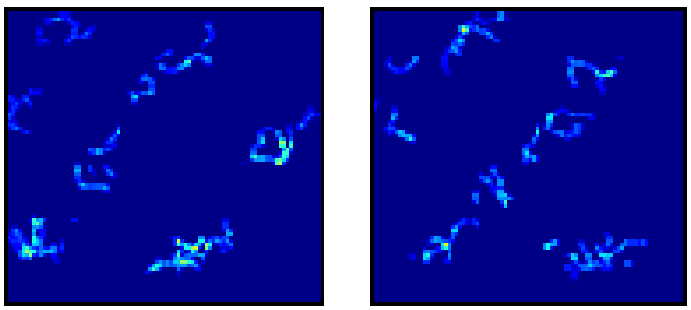

Fig. 4. Averaged activity of 2 simulated grid cells obtained after 1000 steps of random movements (1 step = 2.5 cm) of our animat (≈ 25 m of random movements in an arena of 2 m × 2 m). Each square represents the simulated arena. The discretization of the path integration values is performed on 60 neurons projecting on 10 neurons (defining a modulo 10). Because of the cumulative error in the long-distance path integration neural field, the grid activity shifts linearly on the map and does not appear as a coherent grid on 1000 steps (look like broad lines/only the orientation can be perceived not the spacing). For shorten periods, grids cells can be seen but since only a very small portion of the environment is explored, it is not possible to show some statistics (environment discretization 100 × 100 accumulators).

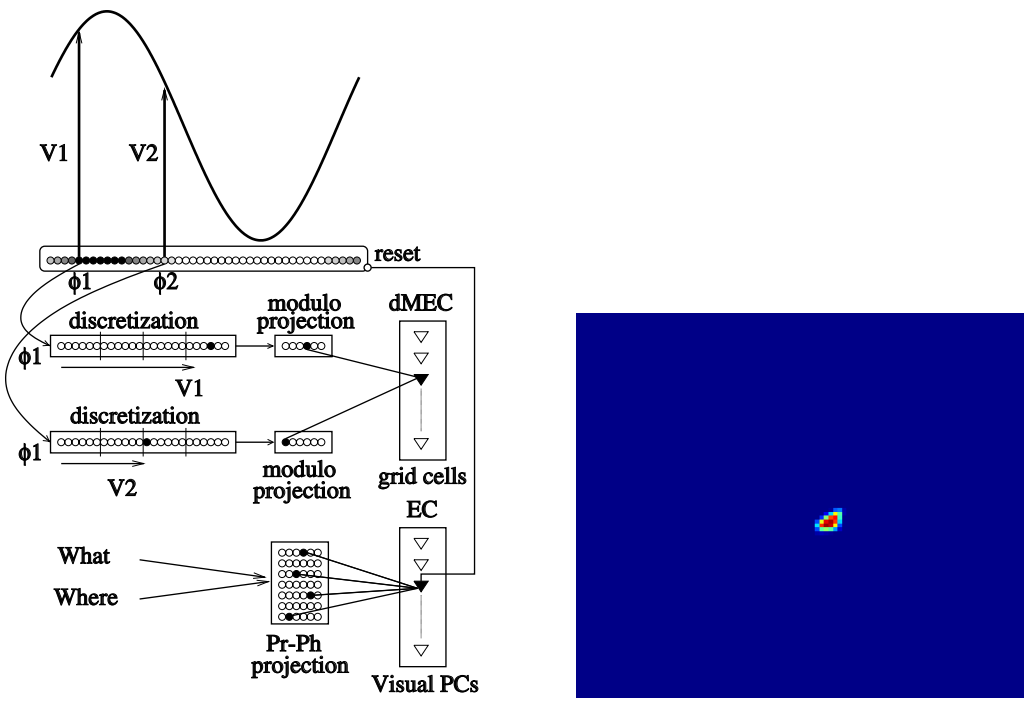

(A) (B)

Fig. 5. (A) Modification of the Fig. 3 to introduce reset or recalibration of the path integration in order to obtain reliable grid cells activities. (B) The recalibration of the path integration to obtain stable grid cell activities takes place when the animat crosses the small activation area almost at the center of the simulated arena. This signal is obtained from the high thresholding of a visual place cell used as a referential (simulated arena of 2 m × 2 m with 8 different landmarks on the borders).

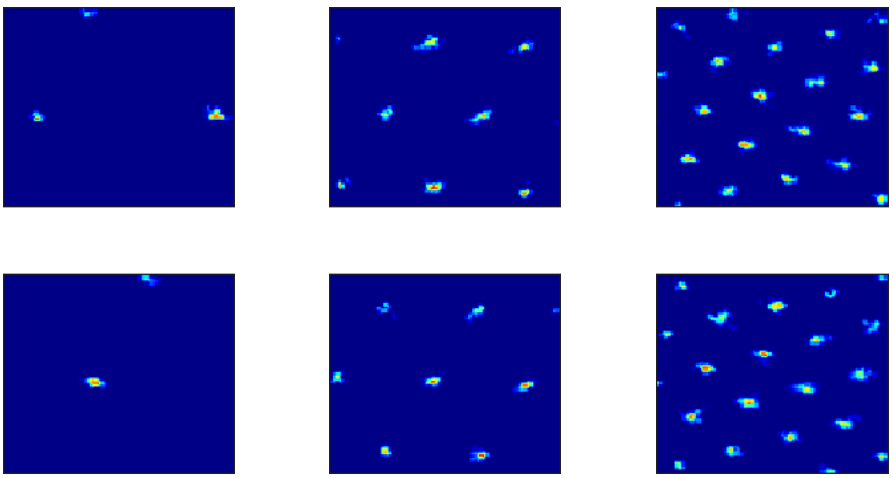

(A) (B) (C)

Fig. 6. Examples of grid cells associated with 3 different values of the modulo allowing to build grid cells at 3 different resolutions (each neuron is exactly connected to 2 fields based on the same modulo). In each column, the activity of 2 simulated grid cells is plotted. 60 neurons projecting on (A) 15, (B) 10 and (C) 6 neurons. The anchoring of the grid activity is controlled by the visual place cell and the network described Fig. 5. Parameters: simulated arena of 2 m $\times$ 2 m, continuous displacement of the animat with a speed of 2.5 cm/iter, statistics computed over 100 $\times$ 100 units.

the activation of the visual place cell triggering the calibration is higher than the recalibration threshold. A second parameter controlling the peak sharpness is the discretization factor of the distance associated with the path integration vector. The sharpness of the grid is limited by the size of the reset area and by the discretization of the path integration distance. Figure 6 shows the activity of three grid cells associated with three different resolutions (three different values of MG: $MG^1 = 15$, $MG^2 = 10$ and $MG^3 = 6$). To obtain narrow and visible grids, the path integration distance was discretized over $N_E = 60$ states corresponding to a maximum distance of above $D_{\max} = 120$ units. If we suppose our arena is 2 m $\times$ 2 m then 1 unit = 4 mm and the 10 000 steps of a simulation correspond to a travel distance about 200 m (see Appendix C for more details on the simulation parameters). The visual recalibration happens around every 500 steps depending on the animat position. It represents a travel of about $5 \times 500 \times 0.004 = 10$ m without recalibration. Other tests were performed on 10 times longer experiments without any change in the results.

A wide variety of grid cell-like activities can be obtained if the neurons learn a given discretized configuration of the path integration neural field (learning and updating equations can be found in B.2). The shape of the fields can be controlled by the number of positions (number of modulo groups) taken in the path integration neural field and the value of the modulo (Fig. 7). When the number of input groups changes randomly from one to six for instance, strange fields may appear as shown in Fig. 8.

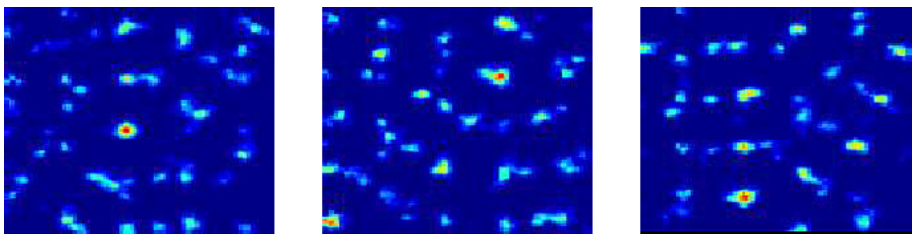

Fig. 7. EC cells with grid cell-like shapes recorded in our simulations when EC neurons learn autonomously configurations from a complete connectivity with inputs coming from 6 fields of neurons associated each to a different value of Φ. Each field corresponds to a discretized angular value of the path integration neural field. Only the potential of the EC neurons is shown (not the final activity after competition since the competition can complexify the pattern of activity and is directly dependent on the number of cells used in the EC model). The maxima of activity correspond to a grid pattern. Secondary maxima with a lower activity (that could be filtered) show the potential details of the periodic pattern. Same simulation parameters as Fig. 6.

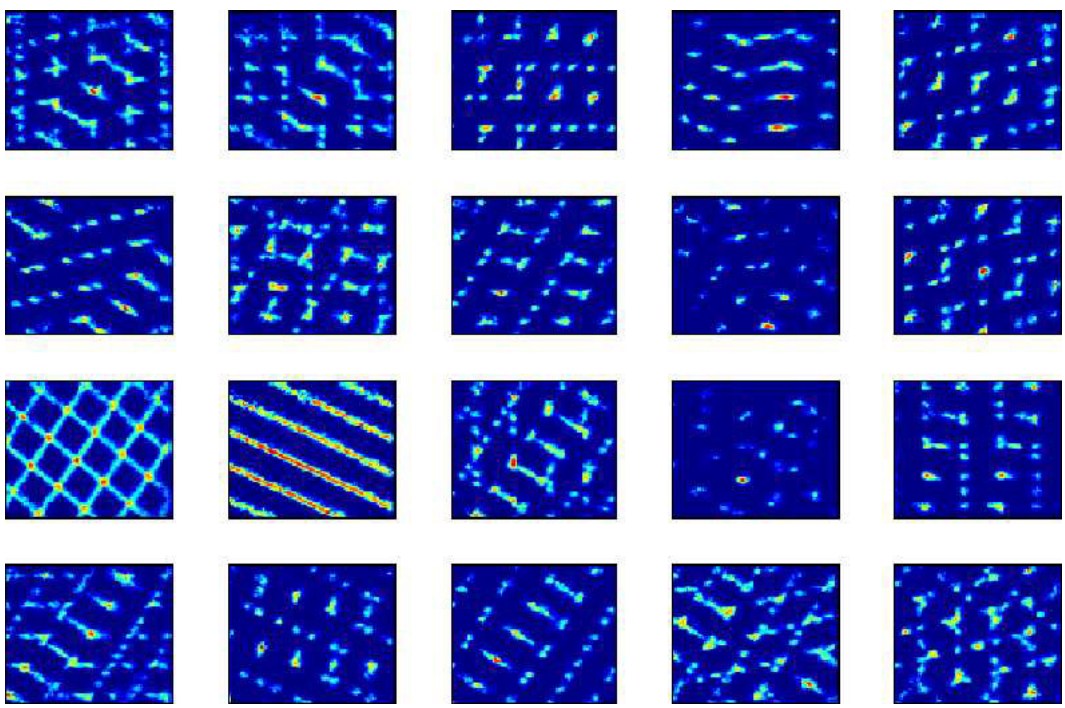

Fig. 8. Modification of the experiment presented Fig. 7. EC cells with grid cell-like shapes or more complex activities recorded in our simulations when EC neurons learn autonomously with a limited and random number of input synapses (here only 50% of chance that an input neuron can be connected and used by an EC cell). Linear activity may appear when the EC neuron is only connected to very few inputs (1 or 2). We represent here only the potential of the EC neurons and not their final activity after competition since the competition can complexify the pattern of activity and is directly dependent on the number of cells used in the EC model. Let's notice that in this cluster of 25 contiguous neurons (randomly selected in a population of more than 1000 simulated neurons) the majority of neurons exhibit a grid cell like activity. Same simulation parameters as Fig. 6.

Our solution is noticeably less restrictive and more efficient than the reset from place to place used in other grid cell models. Indeed, the long-distance path integration used in our model is only discretized along angular values and not distances. In these other models, the maximum error after M steps of displacements is $E_d = \frac{M}{N} \cdot (D_{node}/2)$ with N the number of steps to move from one point to the next on the grid and D_{node} this distance. Note that if N is different from one, then the instantaneous animal speed is not sufficient to move from one point to the next on the grid. A path integration system similar to the proposed one must be added. Yet, in these models, short-distance path integration is reset when the animal arrives to a new point on the grid. It induces a maximum error in distance about $D_{node}/2$ which is not present with our long-distance path integration model since the computation is performed on the analogous values with no reset when entering the next vertex of the grid. There is no error caused by discretization of distance since such discretization is performed only after the output of the computation. Our robotics experiments show that the proposed path integration system can work correctly over several meters. How analogical computations are coded by the brain can be discussed (and is an open question), but many studies on insect navigation show that a pair of analog neurons can do the job quite correctly [43, 44]. It has also be shown that such networks can emerge as a solution of a simulated Darwinian evolutionary process [73]. The main problem with analogous path integration concerns neuron coding precision and the control of activity saturation in the neural network. In the simplest case, we can imagine using a multiscale path integration system comprising several integration modules working in parallel with different integration factors. These modules would be efficient up to a point at which recalibration would be triggered (to avoid the saturation of the neurons). An expected consequence of this system would be a larger grid spacing and an increased field radius (for a constant precision of discretization).

3. Place Cells from Grid Cells and Broad-Field Visual Place Cells

A simple competitive learning, used in our previous work [20, 22, 3], allows building place cells from grid cells (see appendix for the detailed equations — see also [28, 46, 40, 55]). The structure of this network is identical to the one we used to build precise place cells from broad-field visual place cells. A simple online winner-takes-all (WTA) with a selectivity threshold learns particular configurations of the grid cell activity when no other cell is sufficiently active. The resulting activities are place cells with very narrow fields (Fig. 9). A major difference with other grid cell models is that the grid shape is defined neither by predetermined knowledge of the animal's (x, y) coordinates nor by knowledge of the mathematical equation defining the grid shape [63]. All data come from a detailed simulation using only available information similar to that used to control our mobile robots. Path integration information is obtained by simulating the proprioceptive signal stemming from the animat's random movements in the environment.

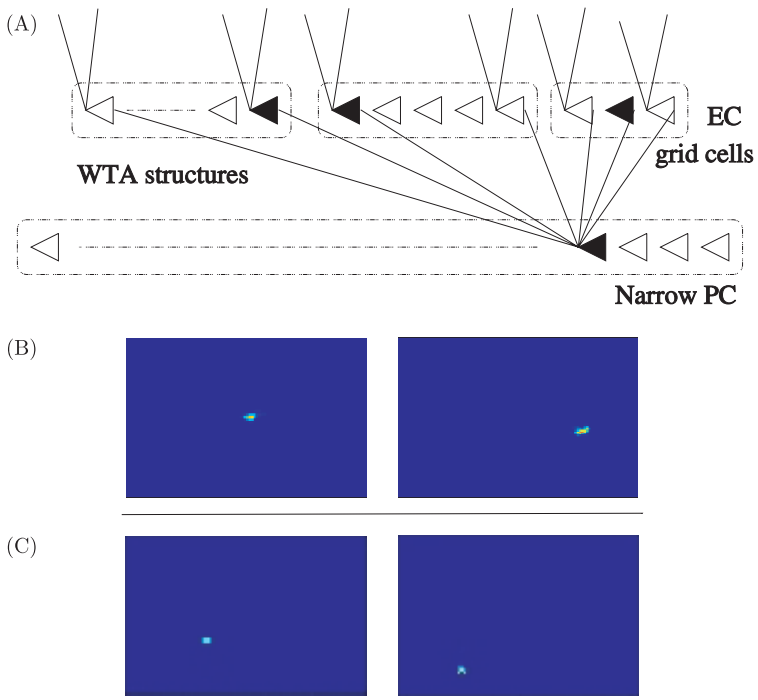

Fig. 9. (A) Simple pattern recognition of activity on several grid maps (with different spacing) allows building sharp place cell activity. Bottom: Representation of the activity of 2 simulated DG place cells. (B) the observed place cells are built from the merging of the 3 maps of grids cells (resolutions 15, 10 and 6 neurons) shown in Fig. 6. (C) similar to (B) but EC visual place cells are introduced as complementary input. (learning parameter vig = 0.3) The two cells have more narrow activity compared to the cells built from the sole grid cells in (B) (other cells have even more narrow activities). Same simulation parameters as Fig. 6.

This model outputs precise place cells. Furthermore, the parameters used to control grid cell activity allow reproducing the variety of neuronal responses found in the literature (spacing, preferred orientation...). Yet our conclusions are very different from those of previous grid cells models since the simulations suggest that a very large population of neurons is required to code correctly the environment depending on the chosen modulos. For instance, with three grids corresponding to a total of $15 + 10 + 6 = 31$ neurons, 2000 neurons (at DG level) were insufficient to code the environment. A key, intrinsic property of our model is that grid cells and the resulting place cells have very narrow fields (because of the discretization of the path integration performed early in the processing chain and because of the loss of topology linked to the modulo operator). Moreover, place cells built from grid cells can have secondary maxima away from the learned location and cannot be used to perform gradient-following (all or none recognition with major risk of failure). On the opposite, EC visual place cells (VPC) can have large fields. As a result, place learning based on the sole grid cells is quite difficult (all places have to be learned with the maximum precision of grid cells) in contrast to learning based on VPC.

Hence, in our model, the granular cells in DG merge both VPC information (from MEC and LEC) and grid cell information (from dMEC) to allow better control of place learning. The richness of the visual signal (abundant, redundant, coherent, robust...) is enough to determine which cell wins the competition. Grid cell inputs are mostly useful when visual information is unavailable or too noisy.

In further simulations, the three groups of neurons coding grid cells (Fig. 6) and a group of neurons coding visual place cells VPC were used as an input for a competitive structure coding DG place cells. To allow both modalities to have nearly identical strengths, the competition mechanism for the choice of the recognized VPC allows a maximum of four winners (the four most activated neurons). Hence, the input to our DG cells is a sparse code of seven activated neurons among a maximum of 861 neurons ($255+100+36$ grid cells + 500 VPCs). Although so few simulated neurons do not allow to manipulate coding sparseness, yet they can be used to verify our theoretical point of view and to extrapolate for other configurations. Figure 10 shows the global pattern of all-to-one connections from the different

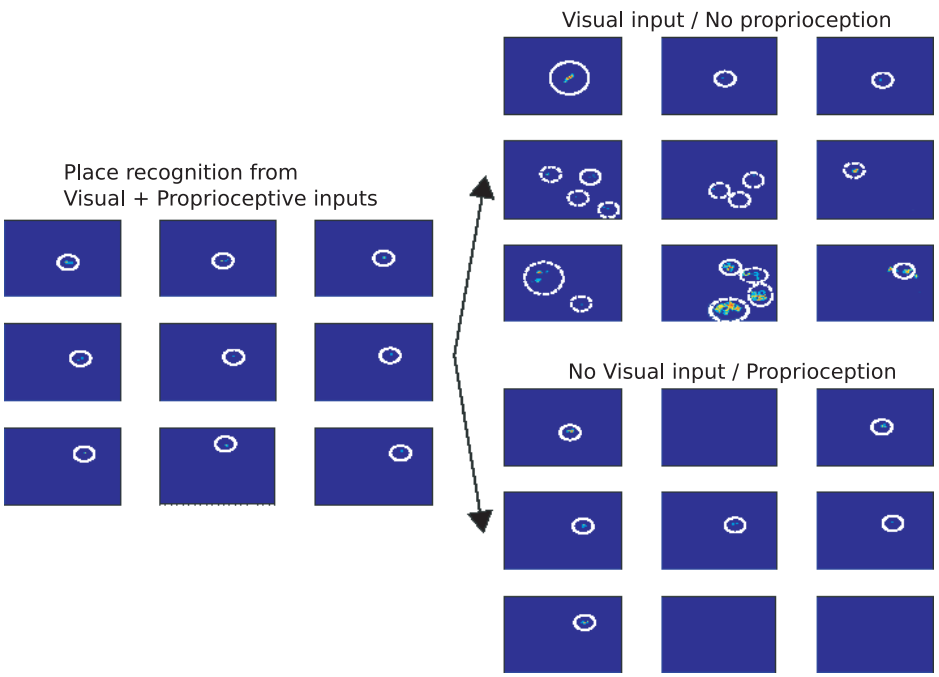

Fig. 10. Left figure shows the activity of 9 place cells learned from the EC activity (population code built from the broad visual place cells and sharp grid cells activities). The input groups are one group of neurons learning the visual place cells with 4 winner neurons over 500 neurons (sparse coding) and 3 groups of grid cells associated to the same resolution as before 15×15, 10×10, 6×6 neurons a single neuron activated on each group of neurons. As a result, the place cells learn a configuration of 7 activated neurons. Right figure up and down shows the activity of the same cells when respectively the path integration signal (and grid cells) or the visual signal (and the visual place cells) is suppressed. Small circles show the areas where the neurons react the most. Dotted lines are used to show the non corresponding areas of activation. (learning parameter vig $= 0.53$). Same simulation parameters as Fig. 6.

inputs to each DG cell that allow to define coherent and sharp place cells. Similar results can be obtained from the sole grid cells or visual place cells (when using a population code made of several visual place cells). The experiment shows that if visual or proprioceptive inputs are suppressed, most DG place cells maintain their response. Obviously, in the very unlikely event of complete inhibition of proprioceptive pathways (and suppression of EC grid cell activity) resulting fields are broader than when vision is suppressed. Presumably, visual inputs allow for accurate generalization thanks to the continuous nature of the landmark azimuth measurement. The greater number of errors in the event of inhibition of grid cells can be explained by the over-generalization of the VPC and the learning of a composite code which does not necessarily guaranty that each VPC subcode allows to define a coherent response alone (this problem does not exist if VPC are used alone since the recruitment of new neurons is controlled by the response level of the previously recruited cells).

4. Discussion

Using the same general principles as those previously used to model visual place cells in the entorhinal cortex [3], we propose a model of grid cells that does not require prior buildup of a Cartesian map of the environment. In our model, new grid cells are simply recruited when no other cell reacts correctly to the current input configuration. This possibility, however, requires the existence of two types of path integration. At the neurobiological level, the existence of several types of path integration is supported, at least partly, by data suggesting that brain areas, such as the hippocampus, parietal and entorhinal cortex are differentially involved in distinct components of the overall process [58, 49, 48].

First, a long-distance path integration (presumably hosted outside the hippocampal system, e.g., retrosplenial and/or parietal cortex) avoids some of the drawbacks of grid cells models based on local, place-to-place path integration. Indeed, a periodic reset and/or a nonlinearity (in case of attractor models) is necessary to decide which node on the grid is activated or recognized from integration of movement as the animat moves from one place to the next on the grid. This nonlinear calculation can produce large errors when the animat moves in a noncanonical direction or at a noncanonical speed according to the sampling frequency of orientation or speed. These errors may be reduced by increasing the number of grids for each *spacing* × *velocity* × *orientation* configuration. Nevertheless, intrinsic connectivity of the EC/subiculum network becomes then quite complex and difficult to manage compared to the present model[d] in which long-distance path integration is simply based on a linear long-term temporal integration. The discretization and the modulo

[d]Note that other models also require periodic connectivity for the modulo operator but they have to manage the merging of the velocity/orientation information and the triggering of reset signal(s) in the same network while in our model these operations are managed independently in distinct subnetworks.

operation are performed only at the output of path integration, which limits error accumulation (in some cases, our long term distance integration process can reduce the effect of the noise — with an unbiased noise for instance). Moreover, in our model, the reset is not a frequent process (it is triggered only at a single place). Another solution would involve continuous soft recalibration based on the learned relationship between place cell activities and the neural field devoted to long-distance path integration.

Second, even if we advocate the need for a long-distance path integration, a short-distance movement integration is still necessary, at least for navigation behaviors, to learn the action associated with a particular transition from one place to another. In our previous work, we proposed that a general function of the hippocampus might be to perform the processing of transitions allowing short-term predictions [59, 25, 2]. Applied to a spatial problem, this transition function would amount to predicting the next position (and associated transition) based on both knowledge of the current position and a short-distance path integration device [54, 22, 3]. This computation supposes both a capability of hippocampal CA fields to predict perceptual transitions and a capability of the subiculum to learn the relationships between perceptual transitions and associated movements in space [62]. In such a model, integration of movements over short distances is reset whenever the animat recognizes a newly entered place (i.e., each time a place transition is detected).

The first report of grid cells [28] led us to examine whether grid cell discharge could be explained by our model of hippocampal transition cells and the hippocampal loop (Fig. 11). As a matter of fact, transition cells in CA3 and CA1 do carry information about movements since places are associated with directions of displacement. Presumably, neurons in the postsubiculum can learn the univocal association between one transition and the corresponding movement (direction with the head direction cells and velocity [47]) using a simple hebbian learning rule. This motor counterpart of the transition cell could be triggered only at the end of the transition (when enough velocity has been integrated). As a result, any transition of a given amplitude and direction would activate the same neuron thus producing a grid cell activity in EC.

We suppose that velocity (whether it is actual or predicted through the hippocampal loop with our CA transition cells) would be integrated in EC_d (deep layers[e] of EC). The competition in EC_s (superficial layer) would allow to obtain sharp grid cells. This model could explain why the activity in the deep layer of MEC shows a conjunctive coding of position, direction, and velocity [57]. Yet, the shape of the multi-peak activity depends on the shape of the place cells. When places are only determined according to the visual place cells (transition triggered when the animal leaves a given place cell), the grid cell pattern resembles more oriented strips than isolated points on a grid (Fig. 12).

[e] EC_d will be associated with layers 5 and layers 6 of EC.

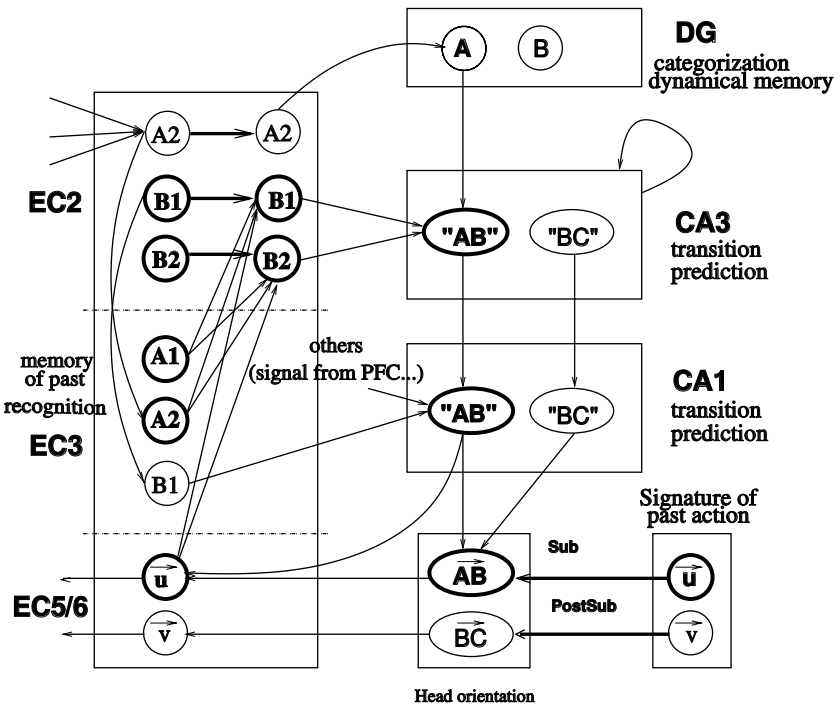

Fig. 11. Model of hippocampal loop applied to navigation (bold circles and ellipses correspond to activated neurons, bold links correspond to unconditional connections). In the superficial layer of EC (EC2 here), incoming information from other cortical areas would allow to build a code characterizing a state (in our case a place). This state is recognized in DG (dentate gyrus). The activity in DG is maintained until a new state is strongly recognized. Hence, CA3 pyramidal cells can learn the correlation between past and present states (respectively provided by DG activity and direct EC2 activity). Theses cells constitute transition cells. The selected transition can be associated in the postsubiculum with the current direction of the animal (linked to its head direction). The short term trace of the previous actions can be stored in the deep layers of EC (EC5/6). We suppose the EC3 layer receives mainly input from EC2 and store the past state of EC2 activity. Hence other neurons in EC2 can learn to predict the activity of the EC2 neurons categorizing the information incoming from other cortical areas according to the previous state (EC3) and the current action (EC5/6). This activity can be either place or grid activity according to the incoming data. The hippocampal loop would not be absolutely necessary to compute place or grid activity but it would bring sufficient data to continue the prediction of the following states in the absence of visual information for instance.

Indeed, the fields of visual place cells cannot be very sharp since small displacements do no induce a large visual displacement of distant landmarks. Moreover, our model entails that the place cell area is defined by a competition mechanism that avoids using *ad hoc* thresholds (which are difficult to manage). Hence place cell fields are stuck to each other so that the winning transition $\overrightarrow{AB}$ is activated for all positions at the border between A and B frontier from A toward B or from C toward $C + \overrightarrow{AB} \ldots$. In contrast, getting a grid cell pattern similar to that observed experimentally (Hafting *et al.*, 2005) would require VPCs to have fields much smaller than in the present simulations. Even if these problems could be solved, computations

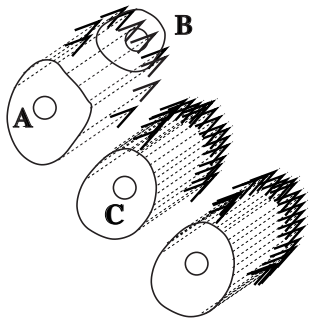

Fig. 12. Shape of the "grid cells" in a model only based on the transition cells to build grid cells. If places are broadly defined (i.e. input from visual place cells) then grid cells should look much more like stripes (i.e. the extremities of the arrows).

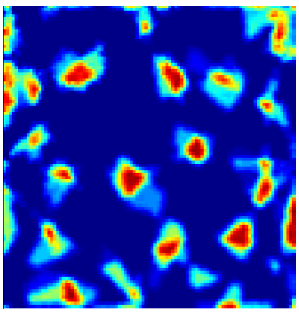

Fig. 13. Activity of a simulated neuron resulting from the thresholded sum of the activities of more than 30 different visual place cells. The spacing of the "grid" diminishes near the borders of the environment (here a rectangular arena) because the relative displacement of the landmarks for a given movement is higher than in the central part of the environment. In open environments, the density of learned places is usually homogeneous. The pattern of activity is somehow similar to the grid cells even if the spacing and the geometry are not as strict as for cells recorded in the dMEC. At the opposite of the dMEC grid cells, the activity of these visual grid cells fades in the dark and it would be complex to build grids of different resolutions at the same time.

based only on visual place cells (see Fig. 13 for an example of a grid cell built from visual place cells) would not explain multi-scale grid cell activity. To do so would require that the learning of visual places in the various regions of EC obeys different rules (e.g., different vigilance parameters) so as to define the different scales. Moreover, we can predict large errors in the noncanonical directions of the grid (a problem similar to that pointed by [6] against [17] model). Yet, closing the hippocampal loop at the level of EC would allow the animat to estimate its current position based on the memory of its previous position and the movement (grid cell activity) coming from the deep layers of EC. Hence after initialization of the system with visual information, it could keep on working in the dark. An internal simulation of a journey could also be obtained using the same mechanism. A possible solution is then to merge the grid cell model built from extra-hippocampal information with the model of grid cells built from computations within the hippocampal loop. Basically, the activity of entorhinal cells would be mainly controlled by the external signal

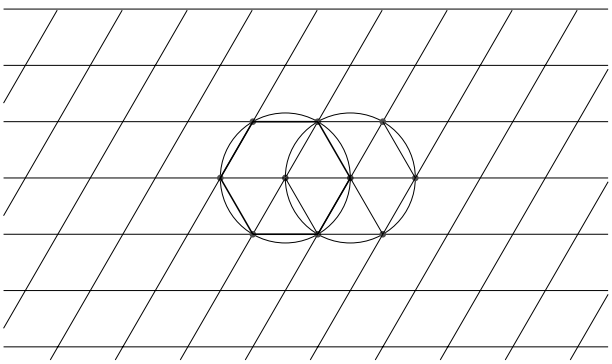

Fig. 14. Paving using a rhombus is equal to a paving made from equilateral triangles. The rhombus paving looks like a hexagonal paving. It corresponds to the superposition of two regular hexagonal paving shifted from half the size of the hexagon.

either visual or proprioceptive and would be combined with the activity coming back through the hippocampal look in case of ambiguity (observability problem) or in the case of the absence of one of the modalities for instance.

Interestingly, the model using the long distance path integration and the modulo operator produces a rhombus paving similar to using an equilateral triangle as proposed by [28] to describe the grid cells (the rhombus is made of two equilateral triangles — see Fig. 14). It must be noticed that this paving is different from the hexagonal paving proposed by other authors. A paving with regular hexagons has the very interesting property of being isotropic. This is not the case with a rhombus paving since it corresponds to the superposition of two hexagonal mapping shifted from the size of the side of the hexagon but the rhombus paving fits very well with the experimental data and allows to build place cells from grid cells. However, in the general case our model predicts rhombus paving but also any other parallelogram paving. To explain the preeminence of a 60° angle between the two orientations of the grids, one simple possibility is to suppose the path integration is stored or decomposed over only six mains directions as it is the case for the visual movements for instance (could also be related to the effect of a lateral competition on a large field). Another possibility could be linked to the conjunction with the visual place cells or simply the more frequent result of the effect of the random selection of more than two orientations to build the grid as shown in Fig. 8. Grid cells build from visual activity tend to have an hexagonal topology (see Fig. 13). Our previous studies [13] have shown the number of possible transitions from one place to the next is between five and six at the maximum. Hence, we can imagine that even with a large set of orientations only those in resonance with the visual place cells could be reinforced.

In summary, we propose a generic model in which there would be a continuous dialog between the entorhinal cortex and the hippocampus: the entorhinal cortex stores and recognizes compressed signatures of cortical activity and the hippocampus proper identifies transitions toward new states, which are fed back to the EC so as to

bias recognition of the new state in the EC. Hence, it would be possible to generalize the proposed network to other modalities such as smell, touch, audition.... The main advantage of our model is that place recognition is nothing but recognition of a multimodal configuration. As a result, updating and maintaining a global and coherent Cartesian map of the environment (based on absolute referential) is no longer necessary since a complete map of the environment inside the hippocampus is not required: a particular compressed path integration vector (and its associated grid cell activities) can be merged with other features (such as visual cues) to recognize a place. The long-distance path integration vector does not need to be coherent when the animal moves over long distances since the memory of its previous activity at a well recognized place can be used to set a new long-distance path integration configuration to help the recognition of the neighboring places.

Finally, it can be questioned if a strict modulo operation is necessary to compress long-distance path integration for grid cell activity to emerge. Ongoing simulations suggest that a low density random pattern of connectivity associated with a competitive learning mechanism can result in a variety of activities including grid cell patterns. Yet, the probability of obtaining regular grids with this mechanism is tiny. Thus, the modulo operation could be essential since it guarantees the emergence of nonambiguous place cells provided relatively prime modulos are chosen. The same process could be generalized to other cortical input of EC to allow for instance better compression, recognition, and prediction of a given cortical activity (although the effect of the modulo operator may be more difficult to detect for nonspatial input). Hence, recent research on grid cells can also help improving models not dedicated to navigation. We hope the robotics tests of the proposed model will highlight the limitations of the present simulations and will allow us to propose new experiments in neurobiology.

Appendix A. A Simple Model for Long-Distance Path Integration

For the long-distance path integration, a simplified neural field without lateral interactions is used (the topology of the field is the same as the topology of the input and the neurons perform only a temporal integration of their input). At each time step, we suppose this field receives an input from the input field coding the direction of the current movement (the information could be provided by the head direction cells of the post-subiculum for instance taking into account the effect of the animal instantaneous speed [69, 68]) To simplify, the size of both fields are supposed to be equal ($i \in 2[0, N]$) with N the number of neurons in each field. The bubble of the input activity V_i is supposed to be centered on the direction of the current movement (the absolute orientation of the animat at time t will be noted $\Phi(t)$). In a first simplified version, its activity has a nonnegative cosine shape:

$$V_i(\Phi(t)) = 1 + \cos(\Phi(t) - \theta_i), \tag{A.1}$$

with $\theta_i = -2\pi\frac{i}{N}$. The neurons D_i in the neural field for path integration simply sum this activity to its own activity (dynamical memory linked to recurrent connections or to the internal dynamics of the neurons).

$$D_i(t) = [D_i(t - dt) + \alpha V_i(\Phi(t)) - r(t)]^+, \tag{A.2}$$

with $r(t)$ is the reset signal, usually null or high enough to reset D_i when necessary (recalibration of the path integration). $[x]^+ = x$ if $x > 0$ and $[x]^+ = 0$ otherwise. α is a gain factor to avoid the saturation of the neural field ($0 < \alpha < 1$). Since the neurons D_i have not lateral connections, their new activity is the sum of all their previous input activities since the reset. The neurons D_i could therefore be considered as a code of the global movement: the direction associated with the winner neuron is the direction of the global movement and the level of activity of this neuron is proportional to the straight line distance (Fig. 15).

Proof. If the animat is moving from 0 (at time t_0) to reach C (at time t_C) with a reset in 0 ($\forall i \in [0, N-1], D_i(t_O) = 0$), the cumulative activity of any neuron i of the field is:

$$D_i(t) = \sum_{t=t_O}^{t_C} \alpha V_i(\Phi(t)) = \alpha\left(\Delta_t + \sum_{t=t_O}^{t_C} \cos(\Phi(t) - \theta_i)\right)$$

$$= \alpha\Delta_t + \alpha \sum_{t=t_O}^{t_C} (\cos\Phi(t) \cdot \cos\theta_i + \sin\Phi(t) \cdot \sin\theta_i)$$

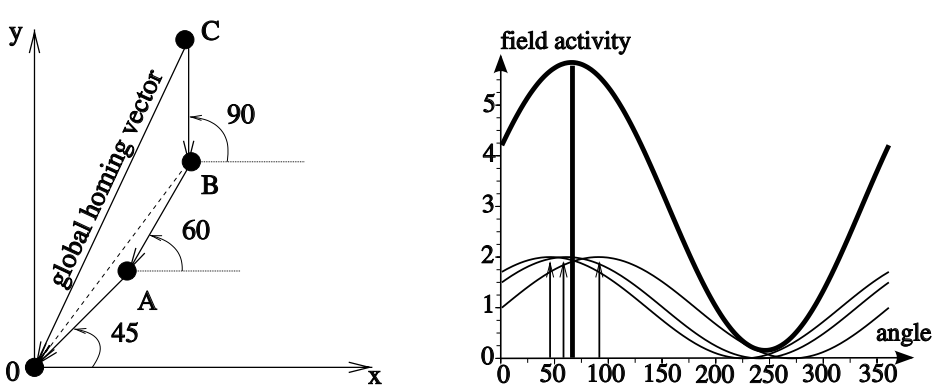

(A) (B)

Fig. 15. An example of path integration. Left figure shows a simulated trajectory composed of 3 movements of the same lenght in the direction 45°, 60° and 90° from an absolute direction. Right figure shows the sum of the associated 3 inputs (neural fields with a cosine shape centered on each movement direction). The sum of the 3 curves (in red) has a maximum activity for the direction of the global movement.

$$= \alpha\Delta_t + \alpha\cos\theta_i \sum_{t=t_O}^{t_C} \cos\Phi(t) + \alpha\sin\theta_i \sum_{t=t_O}^{t_C} \sin\Phi(t), \tag{A.3}$$

with $\Delta_t = T_O - T_C$ (we must have $\alpha < \frac{1}{\Delta_t}$). If we note Φ_T and D the direction and the distance of the straight line displacement from O to C then we have also $D\cos\Phi_T = \sum_{t=t_O}^{t_C} \cos\Phi(t)$ and $D\sin\Phi_T = \sum_{t=t_O}^{t_C} \sin\Phi(t)$. Hence Eq. (A.3) can be rewritten as follow:

$$\begin{aligned} D_i(t) &= \alpha(\Delta_t + D\cos\theta_i\cos\Phi_T + \sin D\theta_i \sin\Phi_T) \\ &= \alpha(\Delta_t + D\cos(\theta_i - \Phi_T)). \end{aligned} \tag{A.4}$$

As a result, the winning neuron in the path integration layer corresponds to the final direction of the movement Φ_T since the last reset of the field activity. Its activity level corresponds to the distance traveled in this direction from the starting point. □

Moreover, the intensity of the neuron associated with the 0 direction corresponds to the global cosine of the movement. It represents directly the distance of the movement projected on the X axis. Conversely, the neuron with the $\pi/2$ direction corresponds to the sine value of the integrated movement (i.e., the projection on the Y axis of the global displacement). Although it is questionable if our brain is able to shape the activity bubbles with the cosine needed for such a path integration mechanism, using a cosine function is only necessary to obtain a mathematically exact result. Any function looking like a cosine, for example a Gaussian function, gives good enough results for path integration. Of course, a small error occurs at each step of the global movement computation. After several displacements, this systematic error could result in a drifted path integration. This characteristic should be compared with experiments performed with ants [75] showing systematic errors in path integration. Such systematic error is also observed in other insects and mammals, including men. This strengthened the idea that the "function" used by animals for path integration is non-trigonometric (see [77] for a study of the effect of the kernel choice on the systematic path integration error as compared to animals path integration errors).

After a certain distance, a saturation must happen and then a precise result cannot be extracted. Yet the direction of the global movement is one of the saturated neurons (and not one of the others). The system becomes very imprecise but it does not stop working. To avoid the saturation problem, a possible solution is to use several rings of neurons associated with different path integration precision depending of the distance associated with a unitary increment of the path integration (short distance to long distance path integration). In the present paper, we only need the hypothesis that a global path integration vector can be computed and coded in a way we can extract on a population of neurons the amplitude of the path integration projected in an arbitrary direction. We will not try to refine the proposed model

since it is not the central part of our model and since there is clearly a need of more biological data to decide between the different possible models to compute and code a global path integration vector. Hence, this network is designed so that each individual movement add only a small activity to the neurons allowing to avoid the saturation for all the possible trajectory in our arena. For instance, if we suppose our arena is two meters large and the elementary step of movement is 2.5 cm and the activity of the winning input neuron is 1 then we can take a weight of $\alpha = 0.001$ to be sure our neurons will not saturate (we must verify $\alpha < \frac{0.025}{\sqrt{4}} = 0.0125$).

The proposed path integration mechanism is routinely used on our robots. It should be noticed that the results are dependent on the trajectory performed by the robot: the errors in path integration mainly occur while the animat is turning because of sliding (the same is also true for animals [50]). Moreover, even if we consider the ideal case of a perfect path integration (no noise on the distance and angle measure), the proposed model introduces errors due to the discretization of the angles. These errors are cumulative and depend directly of the neural field size. Figure 16 shows that the error increases slowly with field containing 241 or 481 neurons but the error can increase quite quickly with a field containing only 61 neurons (resolution of 6° per neurons) for instance. The simulations show the

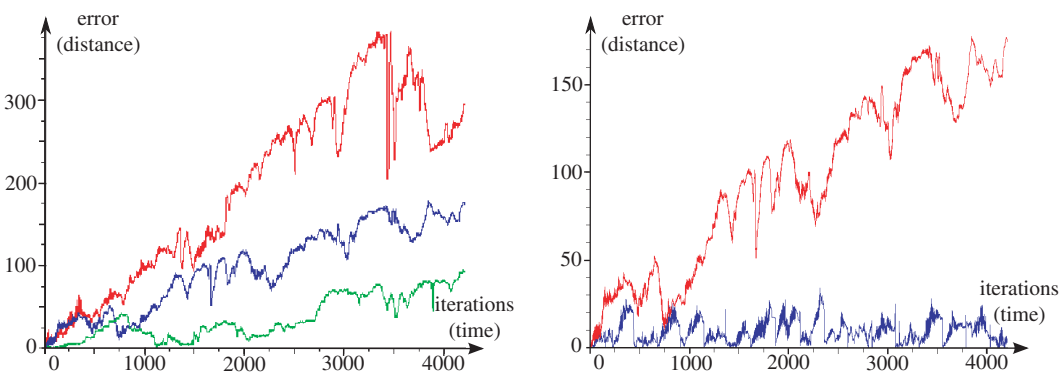

Fig. 16. (A) Study of the impact of the neural field size on the path integration precision. The x axis represents the time in number of iterations of the simulation. The y axis represents the distance between the real position of the robot at time t and the position predicted by the neural field without any reset since the beginning of the experiments (the distance measure is expressed in units: the length of an elementary displacement of the animat correspond to 5 units in the simulated environment). The simulated robot is moving randomly in the 500×500 units arena used for the other simulations (the statistics are summed over 5×5 units squares allowing a display of 100×100 units). (A) The upper curve (higher error) corresponds to a field of 61 neurons, the middle one to a field of 121 neuron and the lower one to 481 neurons (resolution better than 1 degree). (B) (lower curve) Effect of the reset of the path integration neural field triggered by the recognition of a visual place (see Fig. 5). The error remains low and the cumulative effect is limited as opposed to the normal case without reset (upper curve). The test was performed with a neural field containing 121 neurons (middle curve in A)).

coding error increases slowly enough if the number of neurons is higher than 100 neurons. If a narrow place (recognized from visual information) triggers the reset of the path integration (place considered as the origin of the path integration) then the error can be bounded as previously shown by [1] for instance (Fig. 16). Visual information and path integration (or head direction cells) can be merged for solving the drift problem [15] (see [76, 78, 10, 66] for interesting computational models).

Yet, the nature of the neural field used for long-distance path integration can be questioned. As a matter of fact, it could rely on an independent coding of distance and direction[f] as proposed by [11] for visual spatial working memory. The coding of distance could be performed in LIP [30] as well as the modulo operator we need to build our grid cells (see also [5] for the study of visual-vestibular interactive responses in the macaque ventral intraparietal area VIP). Hence, one can suppose the neural field we use for long distance path integration does not really exist but it summarizes or represent in a theoretical way the dynamical interactions between several cortical and sub cortical areas not modeled in this present work.

Appendix B. Equations for Place Learning and Recognition

B.1. *PR-PH activity and learning*

The activity of pattern-encoding PR and direction-encoding PH converged on the PRPH two-dimensional array that merged "What" and "Where" streams to code landmarks by a product (Π or AND operator). All the cells of a column of the PRPH matrix received inputs from the same neighborhood in the "Where" layer. These neighborhoods partially overlapped. Four characteristics of the network deserve to be emphasized: first, although full feedforward connectivity between "Where" and PRPH networks led to accurate performance, PRPH units received only a fraction of "Where" units in order to increase the capacity of the network; second, only maximally active inputs were learned by the PRPH neurons; third, due to input codes, the level of activation of product neurons reflected the angular distance of the corresponding landmark to the current head-gaze direction; finally, assuming that the visual system cannot recognize several patterns in parallel, we use an automatic spotlight system to explore sequentially the visual scene according to a saliency map. This sequential exploration makes "What" and "Where" information temporally correlated and binded. The time-sliced sensory sweep performed by the visual system is corrected by the PRPH working memory which bridges the temporal gap introduced by the sequential exploration (EC delay neurons). The discrete equation of the PRPH neurons activity X_{kl}^{prph} is:

$$X_{kl}^{prph}(t+dt) = \left[X_{kl}^{prph}(t) + I_{kl} - X_{kl}^{prph}(t) \cdot \sum_m In_m \cdot W_{m,kl}^{In-prph} \right]^+, \qquad \text{(B.1)}$$

[f]A direction coding using very few neurons may explain why grid cells with an arbitrary angle are not observed ($0, \pi/3, 2\pi/3, \pi, 4\pi/3, 5\pi/3$ could be the angles used to discretize the directions of displacement).

with $[x]^+ = x$ if $x > 0$ and 0 otherwise. The *excitatory* component of the Eq. (1) includes: I_{kl} a global input to neuron kl detailed below; $X_{kl}^{prph}(t)$, a memory term allowing the build up of a landmark constellation, and fluctuating between 0 and 1. The *inhibitory* term in Eq. (1) induces a reset of the representation of a learned landmark constellation: In_m represents the activity of mth inhibitory interneuron triggered by a sensori-motor reset signal at $\mathrm{T}, 2\mathrm{T}, 3\mathrm{T}, \ldots, n\mathrm{T}$, where T is a constant period for a visual panoramic exploration of the scenery; $W_{m,kl}^{In-prph}$ represents fixed weights between the inhibitory interneuron m and a PRPH pyramidal cell kl. I_{kl}, the global input to neuron kl of the PRPH matrix, is computed as a product.

$$I_{kl} = \left(\max_{i \in N_{li}} L_i \cdot W_{i,kl}^{pr-prph} \right) \cdot \left(\max_{j \in N_{lj}} \Theta_j \cdot W_{j,kl}^{ph-prph} \right) \tag{B.2}$$

$W_{i,kl}^{pr-prph}(W_{j,kl}^{ph-prph})$ are the connection weights between any ith landmark (jth azimuth) input to the kl PR-PH neuron; L_i and Θ_j represent the "What" and "Where" network inputs, respectively. The synaptic weights between input unit j and PRPH neurons learn in one trial a given landmark-azimuth configuration, in absence of inhibitory reset and only for *maximal* input lines:

$$W_{j,ki}^{ph-prph} = (L_i) \cdot (\Theta_j) \cdot f(I - I_n). \tag{B.3}$$

$i = \arg(\max_{p \in N_{li}} L_p)$, $j = \arg(\max_{q \in N_{kj}} \Theta_q)$; I_n is an inhibitory reset activity which prevents learning in case of reset; I is $I = 0.5((\max_{i \in N_{li}} L_i) + (\max_{j \in N_{kj}} \Theta_j))$ with $f(x) = 1$ if $x > 0.99$ and 0 otherwise a thresholded heavyside function, corresponds to a learning modulation common to all active neurons. The Max operator in the previous equations expressed a competition between "Where" neurons belonging to the same neighborhood of inputs to PRPH neurons. Thus, the optimally-tuned "where" neuron could get control of PRPH neuron activation, and learn the corresponding pattern-azimuth conjunction.

In summary, the PRPH network has two functions bind, the "What" and "Where" information in order to create a landmark; bridge the temporal gap between successive landmarks (working memory) in order to create a landmark constellation or view which is directly learned or recognized as a place by EC.

B.2. *WTA mechanism used for EC pyramidal cells and DG granular cells*

The *activity* O_j of an EC pyramidal neuron j (or a DG granular cell in the simplified model used in this paper) is computed as in a Kohonen network [34]:

$$O_j = f_{T_j}\left(1 - \frac{1}{N_i} \sum_{i \in N_i} |W_{i,j} - I_i|\right), \tag{B.4}$$

where I_i is the input and $f_T(x)$ represents an output function that performs a learning-dependent tuning of the neuron response such that the neuron does not

respond before its recruitment (or learning):

$$f_{T_j}(x) = x \quad \text{if } x > 0 \text{ and } T_j = 1 \tag{B.5}$$

$$= 0 \quad \text{otherwise.} \tag{B.6}$$

T_j is used as a simplified version of a tuning factor increased with learning (for instance $T_j = 0$ before learning). A local competition allowing several winners is implemented as follow:

$$O'_j = \begin{cases} O_j & \text{if } O_j = \max_{l/|l-j|<d_{\max}} O_l \text{ and } O_j > vig \\ 0 & \text{otherwise} \end{cases}$$

$d_{\max}$ is a parameter determining the distance on which neurons compete to allow one or several winners on the group of neurons. The learning and recruitment of a new neuron is triggered only if the activity of the winner neuron is inferior to a vigilance parameter vig. In this case ($O'_j < vig$), a neuron k with $T_k = 0$ is recruited ($O'_j \leftarrow 1$ and $T_k \leftarrow 1$) and learns the input configuration:

$$\frac{dW_{ij}}{dt} = \lambda \cdot (I_i - W_j) \cdot O'_j \tag{B.7}$$

with $0 \leq \lambda \leq 1$ a learning factor (in our case $\lambda = 1$ for a one shot learning). If the vig parameter is low, learning is rarely triggered and very few shapes are learned (large distance between the stored patterns in the input space). Conversely, if $vig \sim 1$ the network will learn to differentiate very neighbor inputs. More biologically plausible equations were used in Banquet [3] but the equations used in this paper have been chosen since they provide the same results and they simplify greatly the understand of the computation.

Appendix C. Simulation Parameters

The size of the simulated environment is 500×500 units. The animat position is defined and updated as a floating point number. The instantaneous speed of the animat is 5 units/iteration. The direction of movement is also a floating point number corresponding to the direction of the winning neuron on the motor map. The directions are discretized on a map of 121 neurons (the precision of the angular control is 3°). The discretization of the position is only performed for the graphic display and for the computation of the statistics.

To record the statistics of the neurons activity, the environment is discretized in an array of 100×100 units. The correspondence with metric units could be done easily using a multiplicative factor. Since the parameters used in the simulations allow to control independently each feature of the neurons firing field, there is no real interest to pretend using metric information. Each experiment lasts 10 000 iterations of displacements (excepted the first one which was limited to 1000 iterations to show the neurons activity without a too important blurring of the activity). To avoid disparities between the experiments, a simple homing behavior attracting the

robot on the place used for the path integration recalibration is performed every 400 iterations of displacements (the robot can go to the extremity of the environment before the need to return to the recalibration place is triggered). To simplify the simulations, the place used for the recalibration of the path integration corresponds to the first visual place learned by the robot. Since the robot is put at the middle of the environment at the beginning of each simulation, the same place is used in the different simulations to recalibrate the path integration (Fig. 5).

The simulation of the visual information is very simple. Eight landmarks are regularly distributed at the border of the square environment. Four at the corners and four at the middle of each side. The landmarks are supposed to be perfectly recognized whatever the animat position is. The absolute landmark azimuth is coded on a neural field of only 17 neurons (the angular precision is about 21°). The precision is very small but allows to show graphically the effect of the visual system on the grid cell activity. The simulation of the visual system seems enough precise since real robot experiments show we can obtain qualitatively the same results: the visual place cells in the robotics experiments can use more landmarks (up to 30 landmarks) but suffer from more pattern recognition problems.

Typical value of the vigilance parameter for paving the environment with VPC is $vig = 0.97$. To pave the environment with place cells built from grid cells the vigilance must be drastically reduced ($vig = 0.3$) to avoid the recruitment of a too important number of neurons.

Acknowledgments

The authors thanks the anonymous reviewers for their very useful comments. This work was supported by ACI "integrative and computational neurosciences" and the DGA project No. 04 51 022 00 470 27 75.

References

[1] Arleo A, Gerstner W, Spatial cognition and neuromimetic navigation: A model of hippocampal place cell activity, *Biol Cybern* **83**(3):287–299, 2000.

[2] Banquet J, Gaussier P, Dreher JC, Joulain C, Revel A, Günther W, Spacetime, order, and hierarchy in fronto-hippocampal system: A neural basis of personality, in Matthews G (ed.), *Cognitive Science Perspectives on Personality and Emotion*, Amsterdam, North Holland, Vol. 124, 123–189, 1997.

[3] Banquet JP, Gaussier P, Quoy M, Revel A, Burnod Y, A hierarchy of associations in hippocampo-cortical systems: Cognitive maps and navigation strategies, *Neural Comput* **17**(6):1339–1384, 2005.

[4] Benhamou S, Poucet B, A comparative analysis of spatial memory processes, *Behav Process* **35**:113–126, 1996.

[5] Bremmer F, Klam F, Duhamel JR, Hamed SB, Graf W, Visual-vestibular interactive responses in the macaque ventral intraparietal area (vip), *Eur J Neurosci* **16**(8):1569–1586, 2002.

[6] Burak Y, Fiete I, Do we understand the emergent dynamics of grid cell activity? *J Neurosci* **26**(37):9352–9354, 2006.
[7] Burwell RD, Hafeman DM, Positional firing properties of postrhinal cortex neurons, *Neuroscience* **119**(2):577–588, 2003.
[8] Chadderdon GL, Sporns O, A large-scale neurocomputational model of task-oriented behavior selection and working memory in prefrontal cortex, *J Cogn Neurosci* **18**(2):242–257, 2006.
[9] Charles DP, Browning PGF, Gaffan D, Entorhinal cortex contributes to object-in-place scene memory, *Eur J Neurosci* **20**(11):3157–3164, 2004.
[10] Chavarriaga R, Strösslin T, Sheynikhovich D, Gerstner W, A computational model of parallel navigation systems in rodents, *Neuroinformatics* **3**(3):223–241, 2005.
[11] Chieffi S, Allport DA, Independent coding of target distance and direction in visuospatial working memory, *Psychol Res* **60**(4):244–250, 1997.
[12] Cho J, Sharp PE, Head direction, place, and movement correlates for cells in the rat retrosplenial cortex, *Behav Neurosci* **115**(1):3–25, 2001.
[13] Cuperlier N, Quoy M, Giovannangeli C, Gaussier P, Laroque P, Transition cells for navigation and planning in an unknown environment, *Soc Adap Behav SAB 2006*, pp. 286–297, Rome, 2006.
[14] Dudchenko P, Wood E, Eichenbaum H, Neurotoxic hippocampal lesions have no effect on odor span and little effect on odor recognition but produce significant impairments on spatial span, recognition, and alternation, *J. Neurosci* **20**(8):2964–2977, 2000.
[15] Etienne A, Mammalian navigation, neural models and biorobotics, *Connect Sci* **10**(3–4):271–289, 1998.
[16] Fleischer JG, Gally JA, Edelman GM, Krichmar JL, Retrospective and prospective responses arising in a modeled hippocampus during maze navigation by a brain-based device, *Proc Natl Acad Sci USA* **104**(9):3556–3561, 2007.
[17] Fuhs MC, Touretzky DS, A spin glass model of path integration in rat medial entorhinal cortex, *J Neurosci*, 2006.
[18] Fyhn M, Molden S, Witter M, Moser E, Moser M, Spatial representation in the entorhinal cortex, *Science* **305**:1258–1264, 2004.
[19] Gallistel C, *The Organization of Action: A New Synthesis*, Erlbaum, Hillsdale, New Jersey, 1980.
[20] Gaussier P, Joulain C, Banquet J, Lepretre S, Revel A, The visual homing problem: An example of robotics/biology cross fertilization, *Robot Autom Syst* **30**:155–180, 2000.
[21] Gaussier P, Moga S, Quoy M, Banquet J, From perception-action loops to imitation processes: A bottom-up approach of learning by imitation, *Appl Artif Intel* **12**(7–8):701–727, 1998.
[22] Gaussier P, Revel A, Banquet J-P, Babeau V, From view cells and place cells to cognitive map learning: Processing stages of the hippocampal system, *Biol Cybern* **86**:15–28, 2002.
[23] Georgopoulos A, Neural interpretation of movement: Role of motor cortex in reaching, *FASEB J* **13**:2846–2857, 1988.
[24] Giovannangeli C, Gaussier P, Banquet JP, Robustness of visual place cells in dynamic indoor and outdoor environment, *Int J Adv Robot Syst* **3**(2):115–124, 2006.
[25] Grossberg S, Merrill J, The hippocampus and cerebellum in adaptively timed learning, recognition, and movement, *J Cogn Neurosci* **8**:257–277, 1996.

[26] Grüsser OJ, Pause M, Schreiter U, Vestibular neurones in the parieto-insular cortex of monkeys (macaca fascicularis): Visual and neck receptor responses, *J Physiol* **430**:559–583, 1990.

[27] Guldin WO, Mirring S, Grüsser OJ, Connections from the neocortex to the vestibular brain stem nuclei in the common marmoset, *Neuroreport* **5**(2):113–116, 1993.

[28] Hafting T, Fyhn M, Molden S, Moser M-B, Moser E, Microstructure of a spatial map in the entorhinal cortex, *Nature* **436**:801–806, 2005.

[29] Hartmann G, Wehner R, The antś path integration system: A neural architecture, *Biol Cybern*, 1995.

[30] Hubbard EM, Piazza M, Pinel P, Dehaene S, Interactions between number and space in parietal cortex, *Nat Rev Neurosci* **6**(6):435–448, 2005.

[31] O'Keefe J, Nadel N, *The Hippocampus as a Cognitive Map*, Clarendon Press, Oxford, 1978.

[32] Kalisman N, Silberberg G, Markram H, The neocortical microcircuit as a tabula rasa, *Proc Natl Acad Sci USA* **102**(3):880–885, 2005.

[33] Koch C, Ullman S, Shifts in selective visual attention: Towards the underlying neural circuitry, *Hum Neurobiol* **4**:219–227, 1985.

[34] Kohonen T, *Self-Organization and Associative Memory*, 3rd edn., Springer-Verlag, Berlin, Heidelberg, 1989.

[35] Kolb B, Tees R, *The Cerebral Cortex of the Rat*, MIT Press, 1990.

[36] Krichmar JL, Edelman GM, Brain-based devices for the study of nervous systems and the development of intelligent machines, *Artif Life* **11**(1–2):63–77, 2005.

[37] Krichmar JL, Seth AK, Nitz DA, Fleischer JG, Edelman GM, Spatial navigation and causal analysis in a brain-based device modeling cortical-hippocampal interactions, *Neuroinformatics* **3**(3):197–221, 2005.

[38] Markram H, The blue brain project, *Nat Rev Neurosci* **7**(2):153–160, 2006.

[39] Mataruna H, Varela F, *Autopoiesis and Cognition: The Realization of the Living*, Reidel, Dordrecht, 1980.

[40] McNaughton B, Battaglia FP, Jensen O, Moser EI, Moser M-B, Path integration and the neural basis of the "cognitive map", *Nat Rev Neurosci* **7**:663–678, 2006.

[41] Meyer J, Wilson S, From animals to animats, in Press M (ed.), *SAB91: From Animals to Animats*, Bardford Books, 1991.

[42] Migliore M, Cannia C, Lytton WW, Markram H, Hines ML, Parallel network simulations with neuron, *J Comput Neurosci* **21**(2):119–129, 2006.

[43] Mittelstaedt H, Control systems of orientation in insects, *Annu Rev Entomol* **7**:177–198, 1962.

[44] Mittelstaedt H, Analytical cybernetics of spider navigation, in Barth F (ed.), *In Neurobiology of Arachnids*, Springer, Berlin, pp. 298–318, 1985.

[45] Mittelstaedt H, Triple-loop model of path control by head direction and place cells, *Biol Cybern* **83**(3):261–270, 2000.

[46] O'Keefe J, Burgess N, Dual phase and rate coding in hippocampal place cells: Theoretical significance and relationship to entorhinal grid cells, *Hippocampus* **15**(7):853–866, 2005.

[47] O'Mara S, The subiculum: What it does, what it might do, and what neuroanatomy has yet to tell us, *J Anat* **207**(3):271–282, 2005.

[48] Parron C, Poucet B, Save E, Cooperation between the hippocampus and the entorhinal cortex in spatial memory: A disconnection study, *Behav Brain Res* **170**(1):99–109, 2006.

[49] Parron C, Save E, Evidence for entorhinal and parietal cortices involvement in path integration in the rat, *Exp Brain Res* **159**(3):349–359, 2004.

[50] Poucet B, Benhamou S, The neuropsychology of spatial cognition in the rat, *Crit Rev Neurobiol* **11**(2–3):101–120, 1997.

[51] Quirk G, Muller R, Kubie J, The firing of hippocampal place cells in the dark depends on the rat's recent experience, *J Neurosci* **10**:2008–2017, 1990.

[52] Redish AD, Touretzky DS, Cognitive maps beyond the hippocampus, *Hippocampus* **7**(1):15–35, 1997.

[53] Reeke G, Sporns O, Edelman G, Synthetic neural modeling: The "darwin" series of recognition automata, in Lau C, Widrow B (eds.) *IEEE Proceedings, Special issue on Neural Networks*, IEEE, pp. 1498–1530, 1990.

[54] Revel A, Gaussier P, Lepretre S, Banquet J, Planification versus sensory-motor conditioning: What are the issues? in *SAB'98: From Animals to Animats 5*, pp. 129–138, 1998.

[55] Rolls ET, Stringer SM, Elliot T, Entorhinal cortex grid cells can map to hippocampal place cells by competitive learning, *Network* **17**(4):447–465, 2006.

[56] Samsonovich A, McNaughton BL, Path integration and cognitive mapping in a continuous attractor neural network model, *J Neurosci*, 1997.

[57] Sargolini F, Fyhn M, Hafting T, McNaughton BL, Witter MP, Moser M-B, Moser EI, Conjunctive representation of position, direction, and velocity in entorhinal cortex, *Science* **312**(5774):758–762, 2006.

[58] Save E, Guazzelli A, Poucet B, Dissociation of the effects of bilateral lesions of the dorsal hippocampus and parietal cortex on path integration in the rat, *Behav Neurosci* **115**(6):1212–1223, 2001.

[59] Schmajuk N, A neural network approach to hippocampal function in classical conditioning, *Behav Neurosci* **105**(1):82–110, 1991.

[60] Schöner G, Dose M, Engels C, Dynamics of behavior: Theory and applications for autonomous robot architectures, *Robots Auton Syst* **16**(2–4):213–245, 1995.

[61] Seth AK, Sporns O, Krichmar JL, Neurorobotic models in neuroscience and neuroinformatics, *Neuroinformatics* **3**(3):167–170, 2005.

[62] Sharp PE, Comparison of the timing of hippocampal and subicular spatial signals: Implications for path integration, *Hippocampus* **9**(2):158–172, 1999.

[63] Solstad T, Moser EI, Einevoll GT, From grid cells to place cells: A mathematical model, *Hippocampus* **16**(12):1026–1031, 2006.

[64] Sporns O, Tononi G, Edelman GM, Theoretical neuroanatomy: Relating anatomical and functional connectivity in graphs and cortical connection matrices, *Cereb Cortex* **10**(2):127–141, 2000.

[65] Stackman RW, Herbert AM, Rats with lesions of the vestibular system require a visual landmark for spatial navigation, *Behav Brain Res* **128**(1):27–40, 2002.

[66] Strösslin T, Sheynikhovich D, Chavarriaga R, Gerstner W, Robust selflocalisation and navigation based on hippocampal place cells, *Neural Netw* **18**(9):1125–1140, 2005.

[67] Suzuki WA, Miller EK, Desimone R, Object and place memory in the macaque entorhinal cortex, *J Neurophysiol* **78**(2):1062–1081, 1997.

[68] Taube JS, Place cells recorded in the parasubiculum of freely moving rats, *Hippocampus* **5**(6):569–583, 1995.

[69] Taube JS, Muller RU, Ranck JB, Head-direction cells recorded from the postsubiculum in freely moving rats. ii. effects of environmental manipulations, *J Neurosci* **10**(2):436–447, 1990.

[70] Thinus-Blanc C, *Animal Spatial Cognition*, World Scientific, 1996.

[71] Touretzky DS, Redish AD, Theory of rodent navigation based on interacting representations of space, *Hippocampus* **6**(3):247–270, 1996.

[72] Varela F, Thompson E, Rosch E, *The Embodied Mind*, MIT Press, 1993.

[73] Vickerstaff RJ, Paolo EAD, Evolving neural models of path integration, *J Exp Biol* **208**(Pt 17):3349–3366, 2005.

[74] Wan H, Touretzky D, Redish A, Towards a computational theory of rat navigation, in Mozer M, Smolensky P, Touretzky D, Elman J, Weigend A (eds.), *Proc of the 1993 Connectionist Models Summer School*, Lawrence Erlbaum Associates, pp. 11–19, 1994.

[75] Wehner R, Michel B, Antonsen P, Visual navigation in insects: Coupling of egocentric and geocentric information, *J Exp Biol* **199**:129–140, 1996.

[76] Wiener SI, Arleo A, Persistent activity in limbic system neurons: Neurophysiological and modeling perspectives, *J Physiol Paris* **97**(4–6):547–555, 2003.

[77] Wittmann T, Schwegler H, Path integration — A network model, *Biol Cybern* **12**(73):569–575, 1995.

[78] Zugaro MB, Arleo A, Berthoz A, Wiener SI, Rapid spatial reorientation and head direction cells, *J Neurosci* **23**(8):3478–3482, 2003.